University of California,

Irvine

Challenges in Additive Manufacturing of Alumina

Thesis

Submitted in partial satisfaction of the requirements for the degree of

Masters of Science

In

Materials Science and Engineering

By

Hugo Gonzalez

Thesis Committee:

Professor Martha Mecartney, Chair

Associate Professor Daniel Mumm

Associate Professor Lorenzo Valdevit

2016

Table of Content

Page

List of Figures

Page

List of Tables

Page

Acknowledgements

I would like to acknowledge and thank the following people for their guidance and support while working on this thesis. In no specific order: Dr. Martha Mecartney, Dr. John Halloran, Dr. Biljana Mikijelj, Zubair Nawaz, Stoney Middleton, Jamie Mac, Joshua Cheng.

Thank You!

Abstract of the Thesis

Challenges in Additive Manufacturing of Alumina

By

Hugo Gonzalez

Master of Science in Materials Science and Engineering

University of California, Irvine, 2016

Professor Martha Mecartney, Chair

Additive manufacturing is seen by many as the holy grail of manufacturing, the ability to produce parts nearly autonomously. Adding material rather than removing it would eliminate the need for expensive resources and machining. The recent expiration of key 3D printing patents has led to many advances in the field and has dramatically lowered the prices of 3D printers, making them accessible to the average individual. The one area where additive manufacturing is still in its infancy is in ceramics. Ceramic materials have advantages over polymers and metals such as corrosion resistance, insulating behavior, high stiffness and high temperature stability that make them attractive in industries such as aerospace, medical, and electronics. Processing and machining ceramics however is difficult and expensive as it requires high temperature furnaces and diamond tooling. There are currently two companies that produce printers capable of printing technical ceramics, Lithoz in Germany and 3D Ceram in France. The issue is that both of these printers retail for over $100,000. The work in this thesis intends to show the challenges associated with setting up a ceramic 3D printer at a fraction of that cost for 3D printing of alumina.

The first such challenge was creating a photopolymer resin that could be loaded with a large volume percent of aluminum oxide powder while maintain its curability and low viscosity. Several combinations of monomers and dispersants were evaluated before coming to the conclusion that the

use of a hexanediol diacrylate monomer and quarternary ammonia acetate were the most effective in suspending volume sold loadings of over 40% while maintaining a low viscosity. The next challenge was adapting an inexpensive polymer printer to use the powder loaded resin. Various printer parameters were modified and different window coatings were implemented to create a print. The issue of the layers curing on the build area window however, proved to be difficult to overcome with only partial prints being produced. The conclusion suggest alternative strategies to overcome this problem.

1. Introduction

Additive manufacturing, or 3D printing as it is more commonly called, has long captured the imagination of people and is seen by many as the holy grail of manufacturing [1]. The ability to produce tools, molds, prototypes, and other components by adding material layer by layer rather than by removing it would greatly reduce waste and cost. Waste and cost are huge components in lean manufacturing which many companies aspire to. Additionally, 3D printing would allow for low order or one-off parts to be made at a much lower cost as there would not be a need to create or invest in a new process or tooling. Due to expiring patents of 3D printing technology, the market has now become flooded with 3D printers with several small companies crowd-funding on sites such as Kickstarter [2]. Whereas in the past a 3D printer would cost tens of thousands of dollars, currently there are several options for under ten thousand dollars [1]. This boon in additive manufacturing has primarily been in the area of polymers, with metal printers following behind but still out of the reach of the average enthusiast. The area in which 3D printing is still in its infancy is in ceramics. Ceramic 3D printers have just recently begun entering the market with prices in the hundreds of thousands of dollars [3].

Ceramic materials have unique properties that polymers and metals do not have. Typical ceramics are thermal and electrical insulators which make them perfect for use in electronics such as cell phones [4]. They are also chemically and corrosive resistant which make them ideal for harsh environments where many other materials cannot survive such as inside a human mouth [5]. Finally, ceramics are hard and strong which means they can withstand the toughest applications such as in body armor. For all of these great properties there is one major short coming that has prevent ceramics from widely being used; machinability, for what good does having a perfect material do if it cannot be formed into the necessary shape? Ceramics are extremely difficult to machine, requiring diamond tooling and large amounts of coolant. Designing a complex structure in ceramic such as the one seen in Figure 1.1 would be impossible to create using conventional machining methods. Additionally, the machining

process creates defects in the material, which is detrimental to ceramics as strength depends on flaw size.

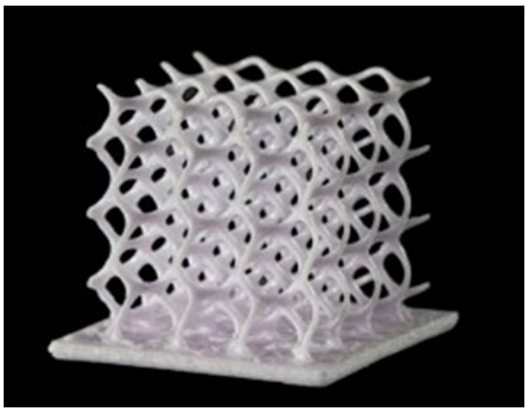

Figure 1.1: Complex ceramic design that would be impossible to machine [41].

The advancement of additive manufacturing in ceramics would allow for complex geometry components, and small parts to be made that would otherwise have been expensive or impossible to machine. The issue with ceramics that separate it from polymers and metals is the melting temperature. The way many of the current 3D printers operate is that they heat the material until it melts, deposits a layer of the melted material, wait for it to solidify before depositing another layer of melted material. This would be very difficult to do with ceramics as most have a very high melting temperature [6]. For all the discussion of printing ceramics being revolutionary, the idea is not a new one, as research has been taking place since the mid-90s, but challenges have limited its development [7].

2. In-Depth Research

2.1 Powder Binder Jetting

The term 3D printing is an umbrella term for various different methods of printing. . In ceramic printing there are currently seven classes that are being developed or investigated. The seven classes are: material extrusion, material jetting, powder binder jetting, sheet lamination, vat photo polymerization, powder bed fusion, and direct energy deposition. Powder binder jetting, laminated

object manufacturing (sheet lamination class), selective laser sintering (powder bed fusion class), and stereolithography (vat photo polymerization class) were selected for in depth research. In powder binder jetting, the system works much like a typical inkjet printer. The ceramic powder is pressed into the build platform and reservoir, both of which move vertically [7]. A roller rolls across, taking powder from the reservoir and pressing it into the build platform. The inkjet heads deposit binder in the shape of the layer being printed. The binder solidifies, binding the powder together, the roller rolls across placing a fresh layer of powder [8]. A typical set-up for the powder binder jetting method can be seen in Figure 2.1.1.

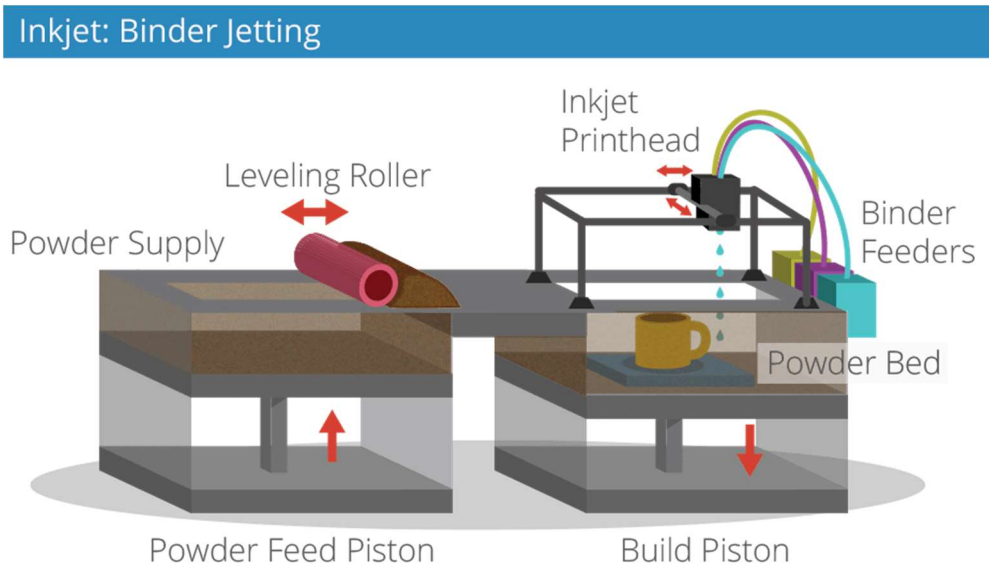

Figure 2.1.1: Typical set-up for a powder binder jetting printer [42].

The key point in achieving a fully dense part using this method is the packing density of the powder in the build platform. The higher the packing density, the higher the green body density will be. Typically ceramics need a green density of at least 60% to fully densify after sintering [7]. The size and the shape of the powder is also extremely important. Fine particles do not flow as well as course particles, producing layers with several defects. Using a course particle size however, negatively impacts the sinter ability of the powder [9]. The amount of binder has to be also taken into consideration. If a small

amount of binder is placed, the green body part would not be able to hold its shape. If a large amount of binder is placed, then the layers would not laminate correctly [7]. Researchers at the Massachusetts Institute of Technology were able to use this method to print alumina with an average density between the parts of 98% and a mean flexural strength between 230MPa and 324MPa [7]. They were able to modify the printer such that instead of using the roller to shear away the excess powder on the powder bed, the piston controlling the powder bed would be slightly raised so that the when the roller would pack the powder [7]. In order to achieve the high densities seen by the team at MIT, post processing techniques would have to be implemented. The method that was used by MIT was cold isostatic pressing the samples after printing. Isostatic pressing refers to application of submerging a part in a liquid and then pressurizing the system so that the part is compacted by the pressure in all directions [10]. It should also be noted however, that the effectiveness of pressing is great for simple shapes, but not as effective for more intricate designs [8]. The other method that could be used was infiltration. In infiltration the printed part is submerged into a bath of a specific solution. The solution would infiltrate the pores in the printed part which was then sintered. In experiments using lanthanum glass and oxidized copper solution as an infiltration, the strength of 64% dense alumina increased from a range of 34-94 MPa to a range of 175-240 MPa [8, 11]. The obvious tradeoff is that the material is no longer phase pure since a second phase is now present. Research has also been performed on infiltration using an alumina slurry, using this method the relative density was increased to 86%. The solid loading of the slurry is dependent on the shape and complexity of the print where more intricate designs require a lower solid loading to penetrate [12].

2.2 Selective Laser Sintering

The next method researched was selective laser sintering (SLS). As the name implies, the ceramic powder is sintered using a high powered laser. SLS was developed by Carl R. Deckard and

Joseph J. Beaman in the 1980s at the University of Texas [13]. The setup is similar to that of the powder binder jetting and can be seen in Figure 2.2.1, the build stage is a bed of powder with a roller that replaces a fresh layer after each layer is printed [14]. The laser system sits overhead where it is directed towards the powder bed using a series of lenses and mirrors. There two different methods of laser sintering that are used, direct and indirect [8]. Using the direct method, the laser heats the ceramic powder to sinter it directly, whereas in the indirect method a secondary powder with a much lower melting temperature than the ceramic powder is heated. The secondary powder is typically a metallic and would bind together the ceramic powder when melted and would have to be sintered to fully densify [8]. Using the direct SLS method, Yttria Stabilized Zirconia was printed with a relative density of 56% [13]. With the indirect method, a thermoplastic was mixed in with the alumina powder. This produced only a relative density of 39%, however after post processing with infiltration and warm isostatic pressing the relative density was increased to 88% [13]. Both of these methods have their inherent issues, the issue with the powder bed packing still persists. It is very difficult to pack the powder into the build platform, thereby decreasing the relative density of the printed part [15]. The laser itself also produces potential issues as the power and scan speed of the laser effects the sintering of the powder [16]. Additionally thermal stresses can develop in the material due to the sintering temperature being upwards of 1500 degrees Celsius and the build platform only being at 200 degrees [13, 15]. With the indirect method, another issue that arises is that the addition of the secondary material would compromised the purity of the material.

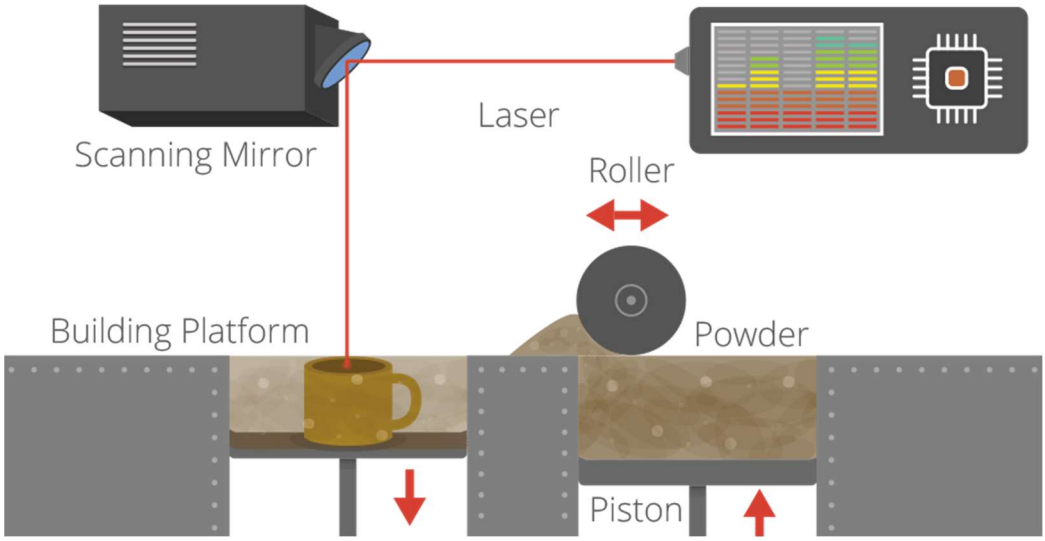

Figure 2.2.1: Typical set-up for a selective laser sintering printer which is very similar to the binder jetting printing method shown in Figure 2.1.1 [42].

2.3 Laminated Object Manufacturing

Laminated Object Manufacturing (LOM) is another method that can be used for additive manufacturing of ceramics. LOM was developed by the Helisys Corporation for initially creating 3D models from sheets of paper, plastic or metal [13]. This method was adapted for ceramic printing by using sheets of ceramic tape. The ceramic tape is rolled over the build stage where an overhead laser cuts the tape into the desired shape. A new layer of tape is rolled over the previous layer and is laminated together using thermoplastic adhesives that are embedded in the tape [8]. A typical set-up can be seen in Figure 2.3.1.

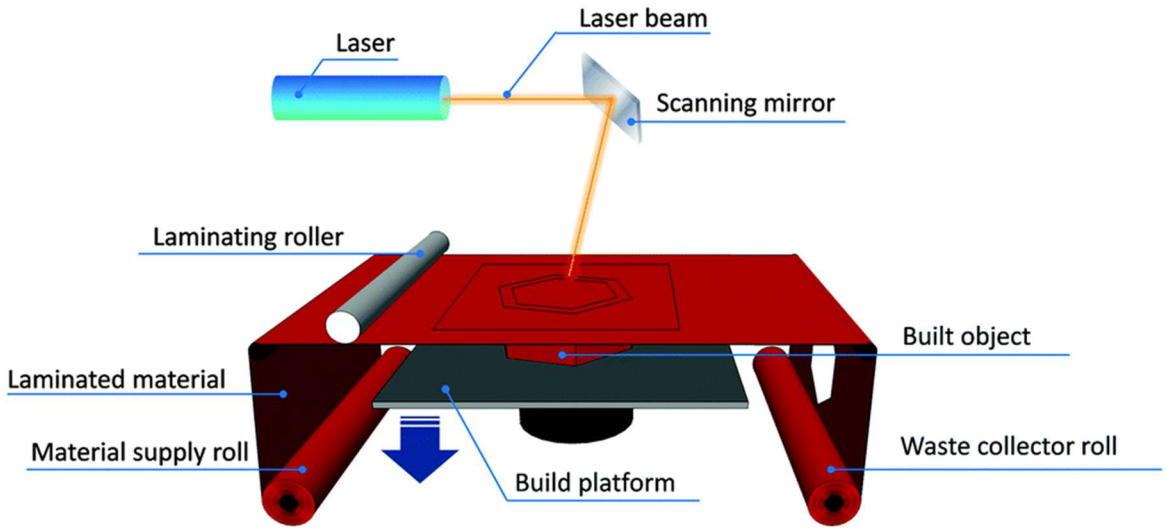

Figure 2.3.1: Laminated object manufacturing printer set-up [43].

The final density is highly dependent on the amount of porosity present in the tape and the pressure at which the lamination occurs [8]. The pressure needs to high enough to pack the particles closely together, however too much applied pressure leads to the formation of cracks in the material. The size of the roller is also important with a bigger roller leading to better lamination between the sheets and a smaller roller having shorter process times [13]. The typical thickness of a ceramic tape is around 200µm. Sintered alumina parts have been printed that achieved a relative density of 99% after post processing [8]. The bending strength of LOM printed alumina was measured at around 311MPa. An experiment alternating alumina and zirconia layers yielded a bending strength of 688MPa [13]. This method has also been applied to other technical ceramics such as Silicon Nitride. A relative density of 97% was achieved from tape cast sheets of silicon nitride with yttria and alumina as sintering aids. The measured bending strength and fracture toughness were measured at 918MPa and 7.5MPa $m^{1/2}$ respectively [13]. It is important to note that LOM does not produce the same type of accuracy as stereolithography or selective laser sintering and is therefore only really used to create models and not finished parts [17].

2.4 Stereolithography

The final method that will be discussed is stereolithography (SLA). SLA was first developed by Charles Hall in 1986 and works by curing a photopolymer resin by exposing it to light in the shape of the layer cross-section [8, 18]. In order to adapt this to print ceramics, ceramic powder needs to be suspended in the photopolymer resin. Ideally one would want to load as much powder into the resin as possible in order to increase the green body density, however there are key aspects that need to be considered. The most important being that the powder remain in suspension. The curing of the photopolymer around the powder is what binds it together, if the resin and the powder separate there would not be anything to bind the powder into the layer cross-section. Additionally the penetration depth of the light must be taken into consideration [19]. The depth of penetration is dependent on the amount of powder suspended in the resin, the particle size, and the index of refraction of both the powder and resin [20]. The more particles there are packed in a given space, the more scattering of light that will occur, thereby decreasing the depth at which the light penetrates [19]. The amount of powder in the resin will also effect the viscosity, which can have varying effects depending on the printer [8]. If a printer relies on the flow ability of the resin to move from the reservoir to the build stage, then having a viscous solution would be ineffective. Research has been performed using this method on alumina and zirconia. Both of these materials yielded a 99% relative density after sintering and strength of 400MPa and 1100MPa respectfully [8]. Bio-ceramics have also been investigated using stereolithography with β-tricalcium phosphate and hydroxyapatite being printed with relative densities of 88% and 95% respectively [21].

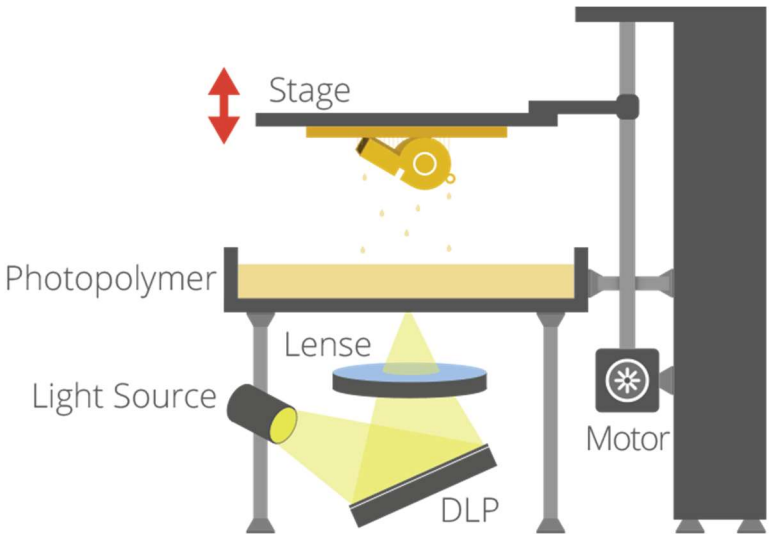

Figure 2.4.1: Stereolithography printer set-up [42].

2.5 Printers in the market

The main purpose of this paper is to outline the challenges encountered when attempting to build a ceramic printer. One of the biggest, if not the biggest, is cost. The binder jetting, SLS, and LOM methods all have printers with costs above $10,000 [22, 23]. In addition to the higher cost, these methods would not produce the densification that was seen on the SLA without the post processing techniques, resulting in more steps and being more expensive. It is for these specific reasons that the SLA was selected as the method to further investigate. Looking into the market, SLA was also chosen as the preferred method by Lithoz in Germany and 3D Ceram in France which have produced SLA ceramic printers. There are two reason why these printers haven't been adopted by the industry, the first being the cost, the Lithoz CeraFab 7500 retails for $250,000, while the 3D Ceram Ceramaker ranges from $100,000 to $250,000 [3, 24]. The second is that the printers are designed to only use the manufacturer's proprietary material, which may not be suitable for the end user application.

Figure 2.5.1: The CeraFab 7500 printer sold by the German company Lithoz retails for $250,000 [3].

Figure 2.5.2: The Ceramaker 3D printer sold by the French company 3D Ceram retails from $100,000 to $250,000 [24].

Stereolithography was selected as the best method for 3D printing alumina, as post processing techniques to achieve high density are not required, and the cost of a printer being less than the other methods.

3. Devices and Materials

3.1 Selecting the Printer

Stereolithography was decided as the best method for experimentation. Several polymer based SLA printers that were on the market were examined:

- Project 1200 by 3D Systems
- Pico 2 by Asiga Freeform
- Max2 by Solidscape
- Form 2 by FormLabs
- 008J by Digital Wax
- B9 Creator by B9 Creations

Immediately the Solidscape Max2 and Digital Wax 008J were eliminated due to their high cost (over $20,000). The evaluated criteria revolved around whether the printer was an open or closed system. A closed system means that the only material that can put in the printer is that which is sold by the manufacturer. The manufacturer places in RFID tag on the material which communicates with the printer and allows it to print [25]. An open system on the other hand refers to a printer that accepts any type of resin. Clearly an open system is desired as a closed system would put a limit on what could be done with the printer. For this reason the FormLabs Form 2 and 3D Systems Project 1200 were eliminated. This left the Asiga Freeform Pico 2 and B9 Creator. Between the two the B9 Creator was roughly half the price in both the unit itself and in the manufacturer's resin. For those reasons the B9 Creator was selected [26].

Stereolithography Printers	B9 Creator by B9 Creations	Project 1200 by 3D Systems	Pico 2 by Asiga Freeform	MAX2 by Solidscape	008J by Digital Wax	Form 2 by FormLabs
Max Build Envelope (mm)	104 x 75 x 203	43 x 27 x 150	51 x 32 x 75	152 x 152 x 101	65 x 65 x 90	145 x 145 x 175
Finest XY Resolution (µm)	30	56	39	10	50	140
Accepts 3rd Party Resins	Yes	No	Yes	No	Yes	No
1kg of Manufacturer's Castable Resin ($)	127	1200	350	700	650	299
Time to Print 5 Castable Models (Hr)	4	6	5	15	8	8
Machine Cost ($)	4,595	4,900	11,990	55,650	26,000	3,499

Table 3.1.1: A comparison of polymer based 3D Printers currently on the market [26]

3.2 The B9 Creator

The B9 Creations B9 Creator was one of the printers that started on the crowd funding site Kickstarter. The printer has a very minimalist design with the only moving parts being the resin vat that moves left to right, and the build table which moves up and down. The vat and build table are enclosed in a UV resistant plastic window. Underneath sits the projector which depending on how it is positioned, is capable of printing in resolutions of 30µm, 50µm, and 70µm [26]. It is also important to note that the printer prints in the blue-light spectrum between 380nm and 420nm [27].

Figure 3.2.1: The B9 Creator printer [26].

The printer relies on the uni-directional motion of the vat to move resin from the reservoir to the build area. Therefore having a resin with a low enough viscosity was very important. A metal sweeper is also attached to the vat which sweeps the resin off the coated build area window. The B9 Creator was attached to a standard PC where the B9 Creator software can be downloaded onto. The software allows one to load .STL file extensions, where size and position can be edited, and supports added. The

viscosity of the B9 Creations red resin would be used as a target was measured at 274 cP using a Brookfield DV-III Ultra Rheometer.

3.3 Almantis A16-SG Alumina Powder

The powder that was used for these experiments was the Almantis A16-SG alumina powder. The mean particle size of the powder was measured at 0.5µm using Horiba Partica LA-950v2 laser scattering system. The specific surface area was measured at 8.5m^2/g using the Micromeritics Flowsorb III 1-Point BET Adsorption. This powder was selected due to its availability, as well as its sub-micron mean particle size. In order to remove any hard agglomerates, the powder was first dried in an oven at 100 degrees Celsius for 1 hour and then passed through a 120 mesh screen. Removing the coarse particles was crucial, as not sieving the powder led to a higher viscosity for the same solid loading.

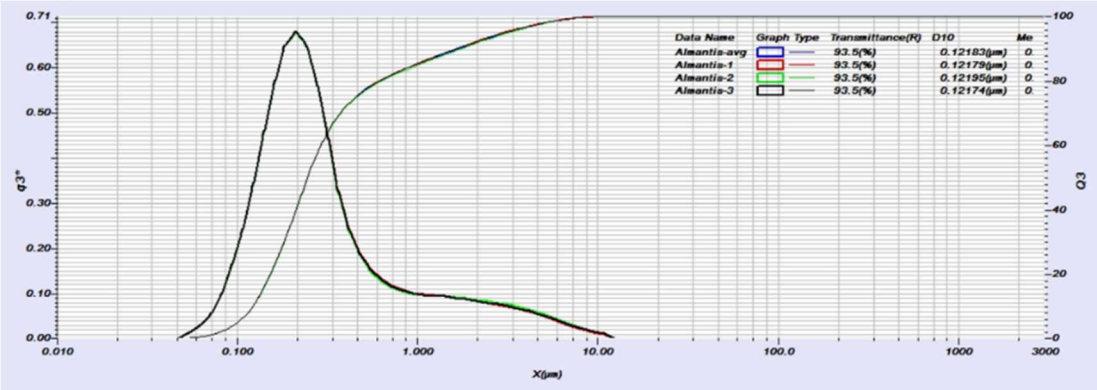

Figure 3.3.1: Particle Size Distribution of Almantis alumina A16-SG performed by a Horiba LA-950v2

3.4 Photomer 4017 and Omnirad BL 751

A photopolymer at its simplest is made up of a monomer and a photo-initiator. A monomer is a small, mostly organic molecule that can bind with other similar molecules to form a polymer [28] a photo-initiator is a compound that converts energy from the absorbed light into chemical energy in the form of initiating species [29]. Without the monomer the photo-initiator would not have anything to

cross-link with, and without photo-initiator the monomer would no cure when exposed to light. The monomer and photo-initiator that would eventually be selected were Photomer 4017 and Omnirad BL 751 respectively. Photomer 4017 was a Hexanediol Diacrylate (HDDA) with a viscosity of 7cP. HDDA was chosen as the monomer based on Dr. Halloran's paper [30]. Omnirad BL 751 was selected based on its compatibility with Photomer 4017 and operating within the printers light spectrum.

The B9 Creator printer was selected as it was the least expensive printer and was an open system. Photomer 4017 and Omnirad BL 751 would be used as the monomer and photo initiator respectively, and the alumina powder that would be used was Almantis A16SG.

4. Experiments

4.1 Manufacturer's Resin Experiments

The first challenge that would have to be met is to create a photopolymer resin with a high solid loading of alumina powder. The work began with the manufacturer's red resin that came with the printer. The resin was specially designed to work with the printer, so it made sense to start there. It was evident that adding powder to the red resin would increase the viscosity past the target of 274cP, therefore work went into manipulating the concentration of the red resin with a low viscous liquid. Three liquids were chosen: water (~1cP), ethanol (~1cP), and isopropyl alcohol (~2cP) [31]. Water was chosen based on its low viscosity, availability and ease to work with. Ethanol and isopropyl alcohol were chosen as a substitute for methanol, as Deckers, Vleugels, and Kruth used methanol as a solvent and dispersant in their photopolymer mixture [32]. Methanol however, is very difficult to work with as it is a toxic substance, therefore it was avoided.

A 1:1 ratio mixture of red resin and one of the three diluting fluids was created to determine how the resins properties would be affected.

Figure 4.1.1: The manufacturer's Red Resin did not mix when placed in water

When the red resin was added to the water, it could be clearly seen that the resin was immiscible as seen in Figure 4.1.1, therefore water was ruled out. Next the resin was mixed with ethanol, and isopropyl. Visually the resin appeared to mix well with both the ethanol and isopropyl, both were poured into an aluminum foil tray and exposed to UV light to determine the effects on the curability of the resin. The ethanol-resin mixture did not cure when exposed to the UV light, the isopropyl-resin mixture cured into a gel-like solid.

Figure 4.1.2: The ethanol and red resin mixture appeared to mix well but did not cure when exposed to UV light

Figure 4.1.3: The Isopropyl and red resin mixture that was cured into gel-like solid

The amount of time it took the isopropyl-resin mixture to cure was much greater than the cure time of the resin alone. While the printer exposure time can be adjusted, it would not make sense to have each layer cure for several minutes. The amount of isopropyl added had to be evaluated to determine how it would affect the cure time. Mixtures of various concentrations; 9:1, 6:1, 5:1, 4:1, and 3:1 red resin to isopropyl were exposed to UV light. The cure time of each was measured with respect to the standard red resin.

Mass Ratio	Volume Ratio	Photopolymer (g)	Photopolymer $(cm)^3$	Alcohol (g)	Alcohol (cm^3)	Total Mixture (g)	Total Mixture (cm^3)	Density of Mixture (g/cm^3)	Cure time w.r.t photopolymer (seconds)
9:1	5.4:1	3.01	2.71	0.39	0.50	3.4	3.21	1.06	0
6:1	4:1	2.06	1.86	0.36	0.46	2.42	2.31	1.05	0
5:1	3.5:1	1.1	0.99	0.22	0.28	1.32	1.27	1.04	19
4:1	2.5:1	1.99	1.79	0.56	0.71	2.55	2.51	1.02	20
3:1	2.1:1	3.18	2.86	1.07	1.36	4.25	4.23	1.01	92

Table 4.1.1: Red Resin-Isopropyl Mixture Curing

It was not until the 5:1 mixture that a noticeable additional amount of time (19 seconds) was needed to cure, with the 3:1 mixture taking a full 92 seconds longer to cure. The 6:1 mixture was selected as it contained the most isopropyl while not affecting the cure time. The viscosity of the 6:1 mixture was measured at 70cP, which was approximately 70% less than the standard red resin. Next, alumina powder was slowly added to the 6:1 mixture until a solid loading of 50 weight % (21 volume %) was reached. A small amount was poured onto a glass petri dish and exposed to UV light. The top layer of the mixture began to cure quickly and uniformly, showing great promise. However, upon close examination it was seen that the majority of the powder has settled at the bottom and that the cured layer contained very small amounts of powder as shown in Figure 4.1.4. Additionally, at only 21 volume % the powder-resin mixture was visually more viscous than the standard red resin. Further changing the concentration of red resin to isopropyl would negatively impact the cure time, nor would it keep the powder in suspension. It was now clear that using the manufacturer's resin would not allow us to attain a high solid loading and low viscosity, therefore a photopolymer would have to be developed in order to achieve the desired results.

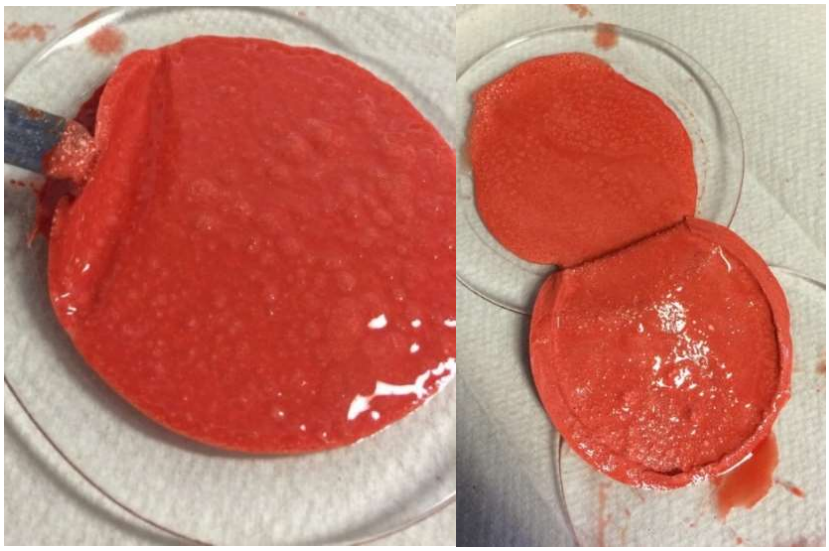

Figure 4.1.4: Cured 6:1 mixture with 50 wt.% powder

The concentration of the manufacturer's red resin was changed by adding isopropyl alcohol to lower the viscosity. While the isopropyl alcohol decreased the viscosity, it also increased the amount of time needed to cure. Additionally the powder would not remain in suspension.

4.2 Photomer 4017 Experiments

From Dr. John Halloran's paper, "Stereolithography of Ceramic Suspensions", it was found that an HDDA monomer and a quaternary ammonium acetate dispersant were able to suspend a high solid loading [30]. After a search for vendors online, IGM Resins was contacted. The sales engineer recommended Photomer 4017 as the low viscosity HDDA monomer and Omnirad BL 751 as a photo-initiator that would work with both the monomer and the printer. The viscosity of Photomer 4017 was measured at 7cP. The photo-initiator was much more viscous, but since only a small amount (less than 1%) is used the viscosity of the mixture is not affected. The Photomer-Omnirad mixture was placed in the B9 Creator and several prints were created with no issues. Additionally the cost of the 2 chemicals were much less than that of the manufacturer's red resin. The IGM engineer however was not able to provide a recommendation on a dispersant as it was not in his area of expertise. Several searches for a quaternary ammonia acetate dispersant yielded no results. The company Dr. Halloran obtained his dispersant, Emcol, was no longer in business, it has been bought out, renamed, and spun off into another company, Variquat, which had made them difficult to find. The victory was short lived however, as the specific product was a special order sample with a sample size of a gallon being offered for the price of $5,000. With that in mind, the search for an alternative dispersant began.

Based on Dr. Halloran's work, an HDDA monomer was sourced from IGM Resins along with a compatible photo initiator. The dispersant used by Dr. Halloran was not acquired based on the cost.

4.3 Silicone Dispersant Experiments

Research was done to learn about the mechanics of a dispersant. The dispersant works by coating the individual powder particles, giving the surface of each particle a charge of the same sign. Since each particle has like charges, they repel from one another. This keeps the particles from agglomerating and sinking to the bottom [33]. Since the goal is to disperse an alumina powder, a search was conducted on dispersants specifically made for it. The sales engineer from Siltech, once again, did not have any specific knowledge on dispersing alumina in a photopolymer resin, but recommended a silicone based dispersant, Silmer ACR A0-UP, based on its effectiveness with alumina powder. A mixture of 90% Photomer, 9% Silmer, and 1% Omnirad was created and the viscosity was measured at 7cP. Two methods would be evaluated for adding the powder and resin mixture. The first would be to slowly add the resin to the powder, while the second would be to slowly add powder to the resin. For the first method, 40g of alumina powder were places into a mixing cup. 10g of the resin mixture were added for volume loading of 50%. The mixture was placed into a high speed mixer at 1600rpm for 1 minute. The results were that the powder agglomerated into several dry, ball-like shapes, which would clearly not work for additive manufacturing.

Figure 4.3.1: 50 volume % loading when mixing the resin into the powder

An additional 8g of resin were added and spun at 1600rpm for 1 minute giving a volume loading of 36%. The resulting mixture was now clumped together to a single dough-like ball, which again would not work for additive manufacturing.

Figure 4.3.2: 36 volume % loading when mixing the resin into the powder

Finally an additional 9g of resin were mixed in and once again mixed at 1600rpm for 1 minute, bringing down volume loading down to 27%. The mixture was more dispersed, but was still clumpy in some areas, and did not flow well.

Figure 4.3.3: 27 volume % mixture when mixing the resin into the powder

In method two, 40 grams of resin were added into a mixing cup. 10g of alumina powder were added and spun at 1600rpm for 1 minute resulting in a volume loading of only 6%. The mixture flowed very well and maintained a milk-like viscosity, but the solid loading was too low.

Figure 4.3.4: 6 volume % loading when mixing the powder into the resin

25g of powder were then added and spun to bring the volume loading to 18%. The mixture had a sour cream-like appearance and still flowed, but it was noticeably more viscous than the red resin.

Figure 4.3.5: 18 volume % mixture when mixing the powder into the resin

A final mixture was created with a volume loading of 27%. This was done to compare method one and two as it had already been clear by the 18% mixture that the dispersant was not working with this system.

Figure 4.3.6: 27 volume % mixture when mixing the powder into the resin

Comparing Figure 4.3.3 and 4.3.6, one can see that adding powder to the resin (Figure 4.3.3) did not produce any agglomerated features as seen in 4.3.6. This meant that the method to combine the powder and resin going forward would be to add the powder into the resin as it led to a better dispersed sample.

Now up until this point the B9 printer had been used to test any of the mixtures, mainly because the mixtures either had a high viscosity or a low solid loading. It was decided to use the printer to attempt to print using a 6 volume % and a 20 volume % Al_2O_3 to determine whether the B9 was capable of handling the addition of the powder. The 6 volume % Al_2O_3 mixture was loaded into the B9 with the standard settings. The resulting print was completed without any issues, however several delaminated strands were hanging from the print as seem in Figure 4.3.7. This was likely caused by the print not

having enough time to settle before the next layer was attached. The main shape of the print however was intact and this complex shape would not have been able to be machined

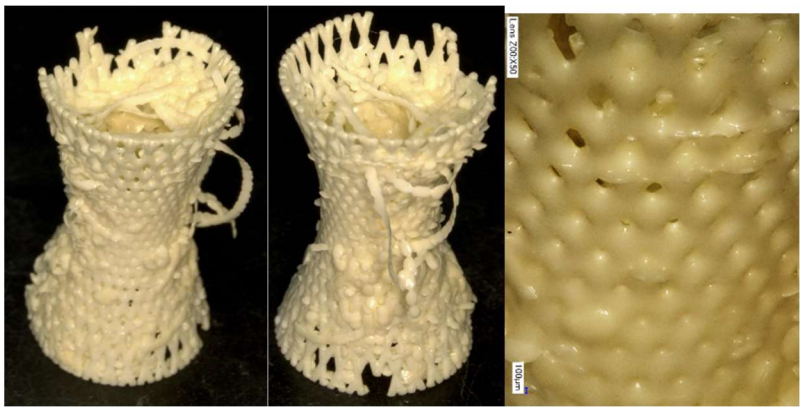

Figure 4.3.7: Printed part made from the 6 volume % Al_2O_3 mixture with the Silmer dispersant. Images taken before binder burn out

The 20 volume % Al_2O_3 mixture was visually much more viscous than the standard red resin. The print was started and immediately it could be seen that it would not be successful. The mixture was so viscous that it would not flow from the reservoir to the build area. Additionally the first layer did cure, but was stuck to the build area window. Both of the 6 volume % Al_2O_3 print and the 20 volume % Al_2O_3 layer that was stuck to the build area window were placed in an oven for binder burn out at 800 degrees Celsius for 1 hour, followed by sintering at 1550 degrees Celsius for 3 hours. The 6 volume % Al_2O_3 print was very brittle, and the shape had become distorted as seen in Figure 4.3.8. The shape of the 20 volume % Al_2O_3 print, seen in Figure 4.3.9, did not distort and could be handled, but strength was still low as the print could be fractured with minimal force.

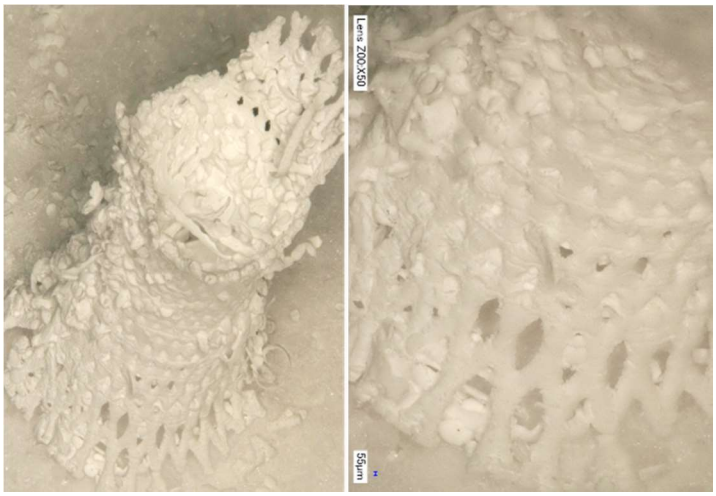

Figure 4.3.8: Sintered part made from the 6 volume % Al_2O_3 mixture with the Silmer dispersant

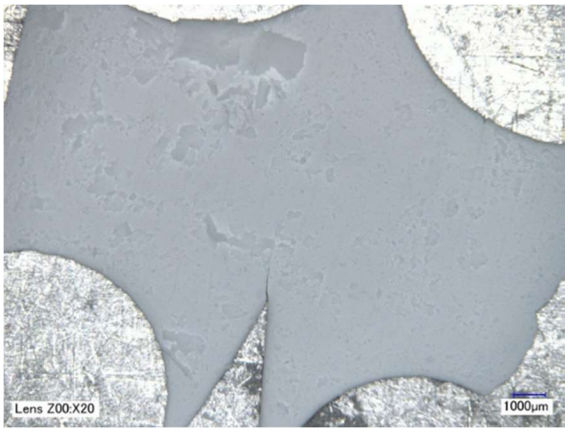

Figure 4.3.9: Sintered part made from the 20 volume % Al_2O_3 mixture with the Silmer dispersant

The 20 volume % Al_2O_3 print was placed into a scanning electron microscope to observe the sintered surface. As expected there was a large amount of porosity in the part as seen in figure 4.3.10. A much higher solid loading would be required to create a fully dense part, and the Silmer dispersant was not adequately dispersing the powder.

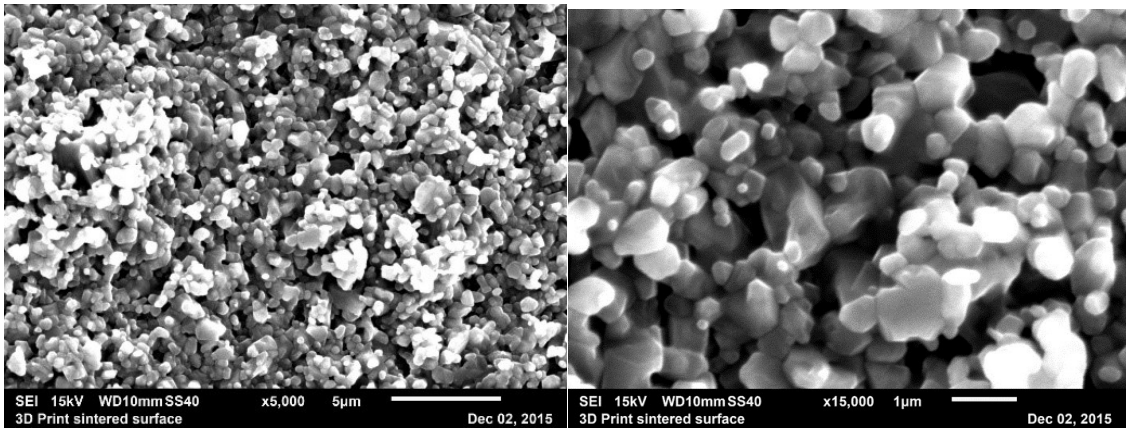

Figure 4.3.10: SEM images of the sintered surface of the Silmer 20 volume % Al_2O_3 mixture. Elevated amounts of porosity could be seen throughout the surface. The grains ranged from 0.17µm to 1.60µm.

The method in which the powder was added to the resin effected the observed viscosity, with the method of incrementally adding powder to the resin producing a lower observed viscosity. The Silmer dispersant was inadequate for high solid loadings of alumina powder, as a volume solid loading of only 20% lead to a cream like consistency that was too viscous for the printer. Parts were printed using the low solid loading mixtures to show that the printer was capable of printing with the Silmer dispersant and powder.

4.4 Polyelectrolyte Dispersant Experiments

Further investigation was done on finding a suitable dispersant to use in the system to increase the Al_2O_3 loading. An internet search of highly loaded alumina suspensions lead to a research paper by Joseph Cesarano III and Ilhan A Aksay titled, "Processing of Highly Concentrated Aqueous α-Alumina Suspensions Stabilized with Polyelectrolytes," that provided helpful information about dispersing high solid loadings of alumina. Cesarano and Aksay state that the pH of the system plays an important role in achieving the high solid loading, low viscosity mixture [34]. Using a polyelectrolyte they discovered that the range of pH that the system would stay in suspension greatly decreased as the solid loading

increased. For solid loading of 20 volume %, the pH range was 4.9 to 9.0, while for a solid loading of 50-60 volume % the pH range shrunk to 8.9 to 9.0 [34]. A sample of Dolapix PC 21, a synthetic polyelectrolyte for dispersing alumina, was ordered from Schwimmer and Zschartz, and two new resin mixtures were created to implement Cesarano and Aksay's findings. Both mixtures consisted of 97% Photomer, 1% Omnirad, and 2% Dolapix. The first mixture was left as is and the pH was measured to be 6, the pH of the second mixture was increased to 9 by adding drops of ammonia to the mixture. Next, 30g of alumina powder were slowly added to both of the mixtures to reach a solid loading of 50 volume % Al_2O_3, both were then mixed at 1600rpm for 1 minute. The powder did not disperse well in either of the mixtures as several large agglomerates visible and the viscosity was visually high. An additional 9 grams of Dolapix were added to both mixtures, lowering the solid loadings to 33 volume % Al_2O_3, and mixed again at 1600rpm for 1 minute. The powder in the 6 pH mixture had separated from the liquid phase and remained agglomerated into a solid block-like shape, shown in Figure 4.4.1. Separation could also be seen in the 9 pH mixture, however the powder appeared to be well dispersed and had high flow-ability compared to the previous experiments, shown in Figure 4.4.2.

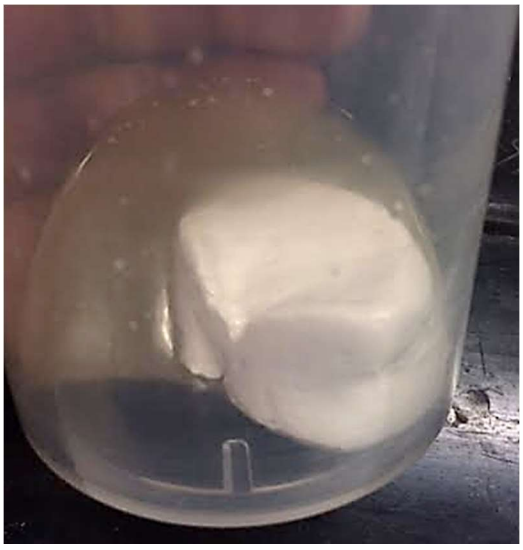

Figure 4.4.1: A 33 volume % Al_2O_3 mixture using the Dolapix dispersant with a pH of 6. The pH was not in the range to disperse the powder. Separation could be seen between the powder and liquid phase.

Figure 4.4.2: A 33 volume % Al_2O_3 mixture using the Dolapix dispersant with a pH of 9. The pH was in the range to disperse the powder. Separation could still be seen between the dispersed powder and the liquid phase.

The excess liquid from the 9 pH mixture was drained out and the remaining mixture was exposed to UV light. No curing was observed as it appears that all of the photopolymer had been separated. The mixture did solidify due to drying, and the pieces was sintered at 1550 degrees Celsius for 1 hour to characterize the density at this solid loading. The density was measured at 3.52 g/cm^3, 88% relative density, by Archimedes method. The piece was placed again placed into a furnace as there were some experimental issues during the sintering cycle. The second sintering cycle was performed at 1600 degrees Celsius for 3 hours. The density was re-measured to be 3.62 g/cm^3, 91% relative density, this of course was much higher than was expected for a 33 volume % Al_2O_3 loaded sample because of the excess fluid that was removed. SEM images were taken of the sintered part which showed much less porosity than seen in Figure 4.3.10, which was the sample with 20 volume % Al_2O_3. The grains were much larger and non- uniform, which was likely caused by grain growth during the second sintering cycle. The grain range for the sample after the first sintering was 0.5µm to 12µm, and 0.5µm to 17µm after the second sintering. The high density is evident compared to the porosity of Figure 4.3.10.

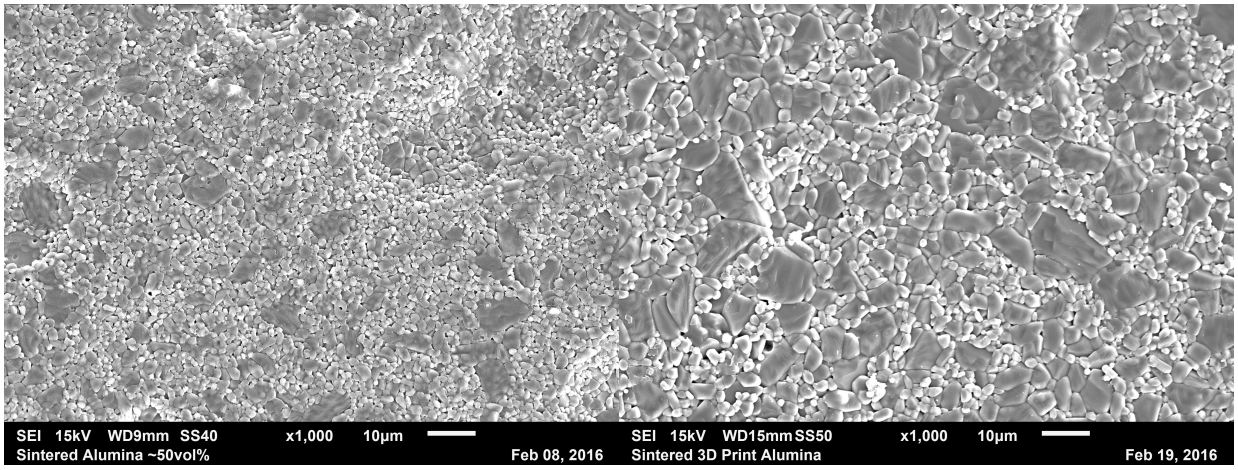

Figure 4.4.3: SEM images of Dolapix mixture part after the first sintering (Left), and after the second sintering (Right). Grain Range for first sintering (Left) was 0.5µm to 12µm and 0.5µm to 17µm for the second sintering (Right).

The pH of the system is very critical to suspending high volume loadings. The acceptable pH range is inversely related to the amount of powder in the system with a 50-60 volume % mixture requiring a pH of 8.9 – 9.0. The polyelectrolyte dispersant was effective in dispersing the alumina powder but was immiscible in the monomer and photo initiator.

4.5 Water Based System Experiment

The separation that was seen was being caused by one of the chemicals not mixing with the Dolapix. All of the alumina dispersants that were found online had one thing in common, they were designed to suspend alumina in water. A 50 volume % mixture of alumina, water, and Dolapix was created to see the effectiveness of the dispersant in water. The mixture was dispersed easily with only hand stirring. The HDDA monomer and the Dolapix were immiscible in each other, therefore causing the separation. A 3M specialist in photopolymer resins recommended switching to a water-dispersible monomer and photo-initiator. This would hopefully alleviate the issue of the dolapix and HDDA

monomer separating. Sartomer SR415 and Irgacure 851DW were specifically recommended. Sartomer SR451 was a water soluble monomer, while Irgacure 819DW was a photo-initiator that was suitable for curing in water based dispersions [35, 36]. The sartomer was on back order and would take several weeks to arrive, therefore ethelyne glycol dimethacrylate was ordered from Sigma Aldrich as it was it was listed as water soluble [37]. The Irgacure was miscible in water, however when the Irgacure-water mixture was added to the EGDA, separation could clearly be seen as shown in Figure 4.5.1.

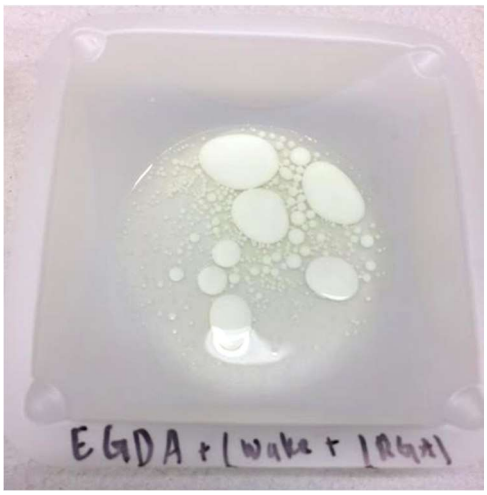

Figure 4.5.1: Separation seen between the Irgacure mixture (white spots) and the EGDA monomer.

A water based monomer and photo initiator were used along with the Dolapix polyelectrolyte. The EGDA monomer proved ineffective as it was immiscible in water and the photo initiator. Sartomer SR415 was not tested as it did not arrive on time.

4.6 Quaternary Ammonia Acetate Dispersant Experiments

On March 4, 2016 Dr. John Halloran visited the University of California, Irvine to give a guest lecture on additive manufacturing, and he offered to send me a sample of Variquat CC-55, a quaternary ammonia acetate that was very similar to the one was used in his research.

A new mixture was created using the variquat dispersant in the following quantities: 42g of Almantis A16SG, 10g of photomer 4017, 2.4g of variquat cc-55, and 0.05g of ominirad 751bl. This gave a solid loading of 46 volume % Al_2O_3. The mixture was then placed in a ball mill overnight. The resulting mixture was well dispersed and flowed well, but the viscosity was still measured at 1051cP. The mixture was then exposed UV light, and almost immediately the top later began to cure, shown in Figure 4.6.1.

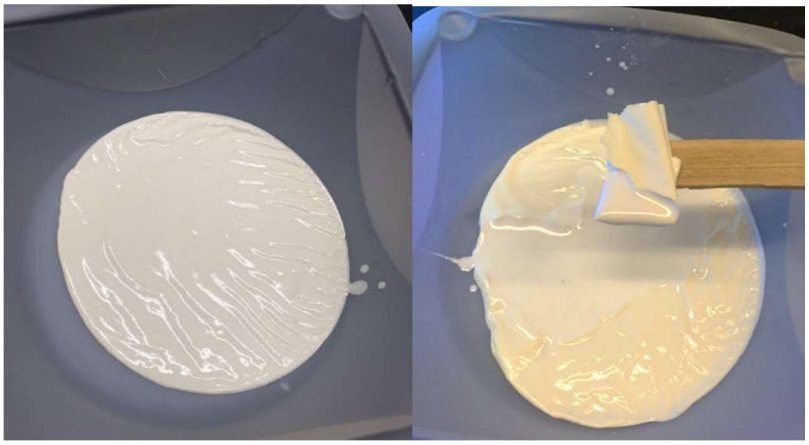

Figure 4.6.1: Cured layer of the Variquat 46 volume % mixture.

A second mixture was made consisting of 45g of powder, 15g of photomer, 2.4g of variquat, and 0.05g of omnirad. This would give a solid loading of 40 volume % Al_2O_3. The mixture was then mixed by hand instead of using the ball mill. The viscosity of the resulting mixture was measured at 358cP. The solid loading was then increased to 47 volume % by adding 10g of powder. The viscosity jumped to 1017cP.

The 40 volume % Al_2O_3 was lower than the targeted solid loading, but it was the highest attained with a viscosity near that of the standard red resin. A larger batch was made to use in the B9 printer. Three batches each containing 100g of powder, 31g of photomer, 6g of variquat, and 0.15g of omnirad were created and then mixed together. The viscosity of the resulting mixture was 506cP which was higher than the 358cP that was expected. The same chemicals and ratios were used in the small and large batch so the issue was most likely that the larger batch was not mixed well enough. The mixture

was placed into the high speed mixture at 1600rpm for 1 minute. Due to the mixing the viscosity of the mixture was reduced from 506cP to 281cP which was nearly identical to the manufacturer's red resin.

A sample of variquat c-55 dispersant provided by Dr. Halloran proved effective in dispersing the alumina powder while not negatively effecting the cure time. High speed mixing was required in order to attain a viscosity reading of 281cP for a 40 volume % Al_2O_3 loaded sample.

4.7 Printing Experiments

The time had finally come to place a high solid loading resin into the printer. The 40 volume % mixture was placed into the B9 printer with the goal of printing a simple cube. The standard settings were used to begin the print. The first few layers of the print were observed, and it was noticed that the layer had stuck to the build area window instead of the build stage. It was mentioned by Dr. Halloran that the crosslinking reaction of the photopolymer is much slower with the added powder. Under the same exposure setting, alumina powder loaded photopolymer cured about 3-5% whereas the photopolymer had cured 75% [30]. The base exposure settings on the B9 printer were increased from about 3 seconds to about 6 seconds, the over exposure was increased to from about 1 second to 2 seconds. The over exposure setting refers to the time the printer takes to cure the edges, while the base exposure is the time it spends curing the rest of the layer. Even after doubling the exposure setting the layers could still be seen sticking to the build area window. The exposure settings were increased again to 9 seconds for the base and 4 seconds for the over, but the issue still persisted. The exposure settings were increased yet again, this time to about 16 seconds for the base and about 8 seconds for the over. The first 10 layers were observed with no sticking to the build area window. The print was then left unattended as it would take several hours to finish. Upon returning halfway through the print, the printer vat could be seen making short jerking motions that had not been observed before. The print

was cancelled as it was assumed that there was an issue with the printer that was preventing the vat from making the full motion. When the build stage was raised from the vat, a small cube could be seen stuck to the surface as shown in Figure 4.7.1. A new print was restarted, however the layers could be seen sticking to the build area window almost immediately.

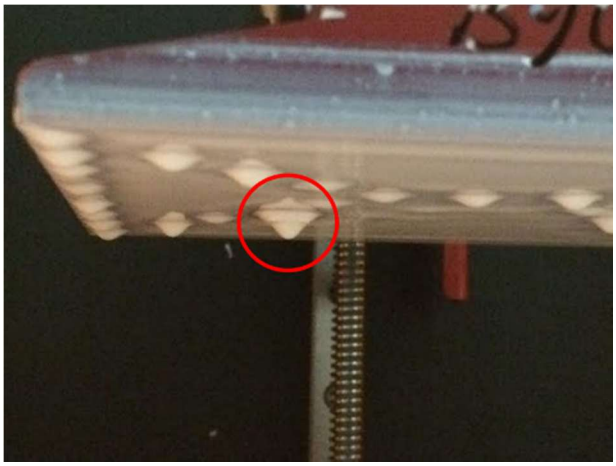

Figure 4.7.1: Image showing the print successfully sticking to the build table.

The resulting failed print had the following dimensions:

- Width: 6.345 mm
- Length: 6.170 mm
- Thickness: 1.622 mm
- Mass: 0.1216 g
- Density: 1.92 g/cm^3

The next step would be to perform a binder burnout on the print to remove the unwanted polymer. We wanted to know at what temperature we would need to reach in order to burn off all of the photopolymer, therefore a thermogravimetric analysis was performed. A sample of the 40 volume % mixture was placed into the Setaram Setsys Evolution 1750 TGA with the following heating cycle:

- Temperature Range: 25 to 800 degrees Celsius

- Heating Rate: 5 degrees Celsius per minute
- Hold: None
- Atmosphere: Air

Based on the TGA results, the photopolymer was completely burned away by 450 degrees Celsius. The printed cube was then placed into a furnace with the following heating cycle:

- Temperature Range: 25 to 500 degrees Celsius
- Heating Rate: 5 degrees Celsius
- Hold: 1 hour

The cube was brittle after the burnout. The weight, width and length were measured. While attempting to measure the thickness, the cube crumbled in between the micrometer. The thickness however, was estimated using the shrinkage factor of the width and length, which was 7%.

- Width: 5.91 mm
- Length: 5.76 mm
- Thickness: 1.51 mm
- Mass: 0.0812 g
- Density: 1.59 g/cm^3

The relative density was calculated to be 40%, which was exactly where it was expected to be. SEM images of the surface of the crumbled cube showed large powder particles scattered throughout the material, porosity could also been seen as expected from an un-sintered part.

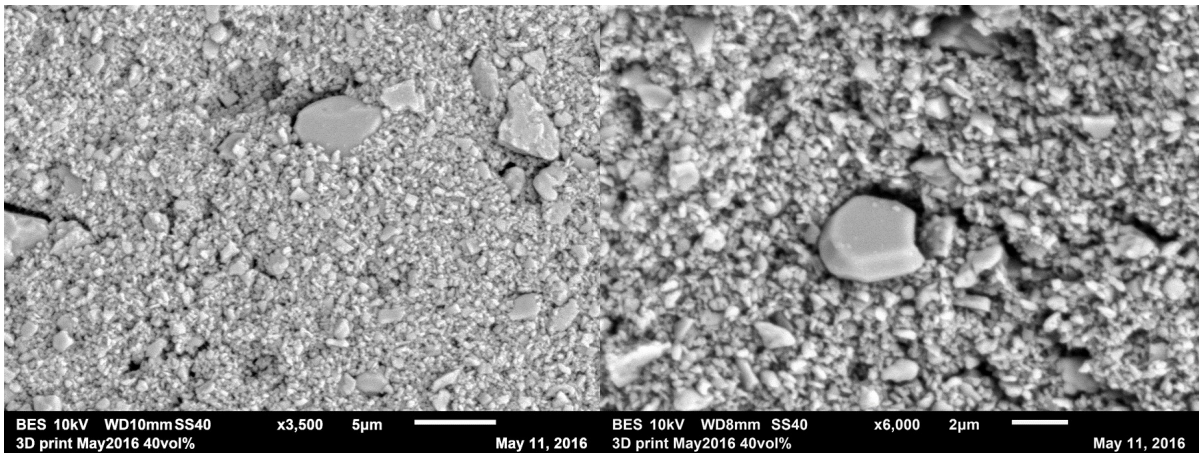

Figure 4.7.2: SEM images taken of the printed cube after binder burnout

In order to help combat the issue of the layers sticking to the build area window, the build table was re-calibrated and the PDMS, polydimethylsiloxane, coating on the window was replaced. The PDMS is an organic silicon based polymer that is placed on the build area window to prevent layers from sticking to it [38]. The PDMS layer needs to be re-oxygenated after each layer to remain effective, this is accomplished by having a sweeper sweep away the resin from the build area window after each exposure cycle. The breath setting on the B9 printer controls the amount of time the printer waits after the sweep to resume printing. None of these changed seemed to help as the layers were still sticking to the window instead of the build stage. Further increasing the breathe time proved ineffective as the resin would flow back to cover the window immediately after the sweep. Increasing the base and over exposure times also did not seem to alleviate the sticking issues. Perhaps the issue was that the individual layers of 30µm were too thick. Therefore the layer thickness was decreased to 10µm and a new print was started. The first 6 layers were observed with no evidence of sticking to the build area window. The print was paused in order to see if the layers were building on the build stage. After 6 layers with a layer thickness of 10µm, the print could be seen adhered to the build stage.

Figure 4.7.3: Printed layers stuck to the build table. The layer thickness was set to 10µm.

The print was resumed unattended. Upon completion however, the print was no longer adhered to the build stage. Additionally, cured layers could be seen stuck on the build area window. Sifting through the resin mixture the unfinished print was found. Based on what was observed, the likely issue was that at some point during the printing process the print broke free from the build stage. This meant that any new layers could not attach themselves to it and where therefore stuck on the build area window instead. The printer parameters were changed so that the build stage would increase its distance between the build area while the vat moved to refresh the PDMS layer with hopes that the increased distance would minimized the chances of the print hitting something and dislodging itself. The print was restarted with the same layer thickness of 10µm, yet in the first couple of layers it could be seen that there were sticking issues. The layer thickness was further reduced to 5µm, and the first 35 layers were observed with no issues. The printer was paused to ensure that the print was in fact on the build stage before resuming. The print however had to be canceled as the printer had stalled due to the build stage getting caught on the PDMS layer. Subsequent prints using the same parameters showed sticking issues on the build area window as seen in Figure 4.7.4.

Figure 4.7.4: Cured layer sticking to the build area window.

Four failed prints were salvaged from the vat and placed into an oven for binder burnout using the following cycle:

- Temperature Range: 25 to 500 degrees Celsius
- Heating Rate: 5 degrees Celsius per minute
- Hold: 1 hour
- Temperature Range: 500 to 1000 degrees Celsius
- Heating Rate: 5 degrees Celsius per minute
- Hold: 30 minutes

The secondary step from 500 to 1000 degrees Celsius was added to bisque the material. This would give it more structural rigidity and allow it to be handled without crumbling as was seen on the previous part. The prints were then sintered using the following heating cycle.

- Temperature Range: 100 to 1600 degrees Celsius
- Heating Rate: 5 degrees Celsius per minute
- Hold: 3 hours

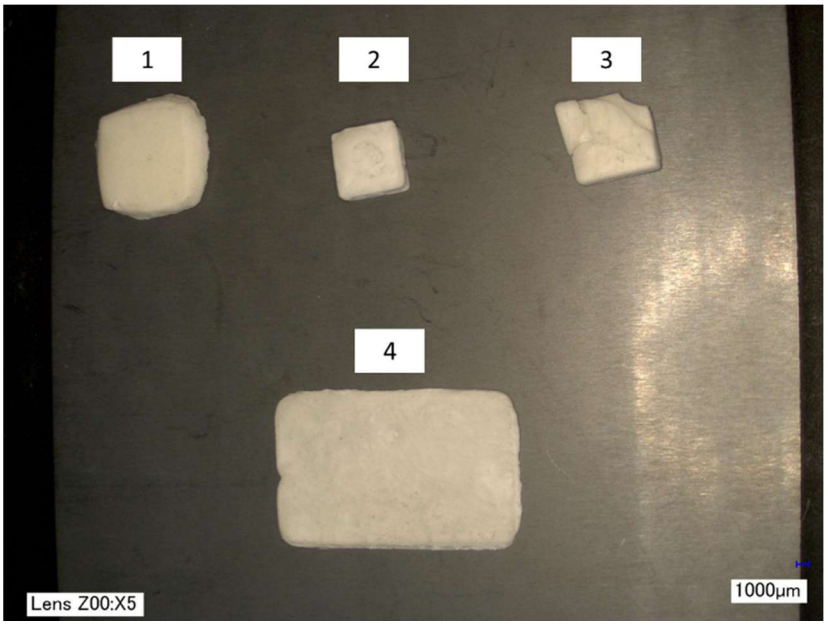

Figure 4.7.5: The four failed prints that were evaluated.

The density of the 4 prints were measured using Archimedes Method.

Print	Density ($g/cm^{3)}$	Relative Density (%)
1	3.44	86
2	3.06	77
3	3.55	89
4	3.73	94

Table 4.7.1: Measured Densities of failed prints.

All 4 of the prints did not contain any open porosity, as they did not take in weight when submerged in water. There was a wide range in terms of the relative density, but the 94% was very promising considering the initial mixture only had a solid loading of 40 volume % Al_2O_3. Prints 1 and 4 were imaged using an SEM. The microstructure between the 86% and 94% relative density prints were very similar with the exception of cracks seen on the surface of print 1.

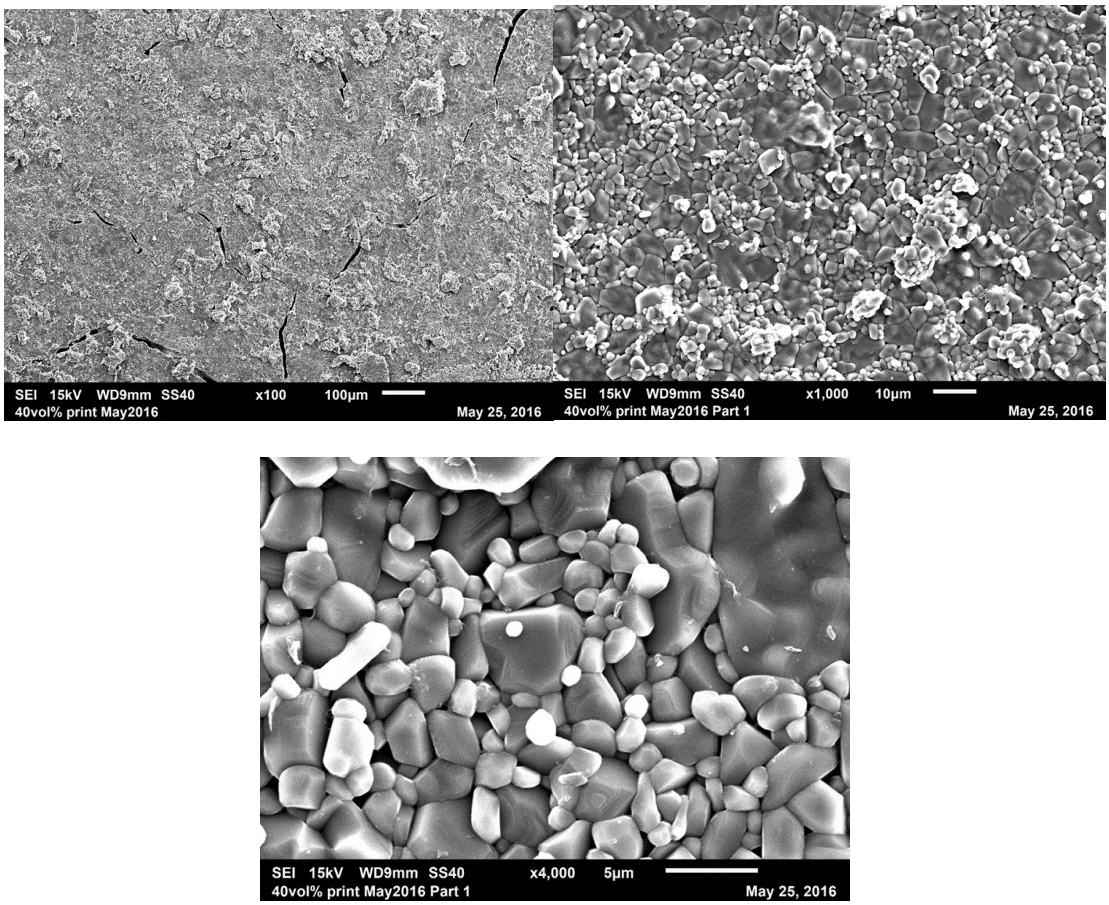

Figure 4.7.6: SEM Images of print 1 (86% relative density). Grain range measured 0.75µm to 20µm.

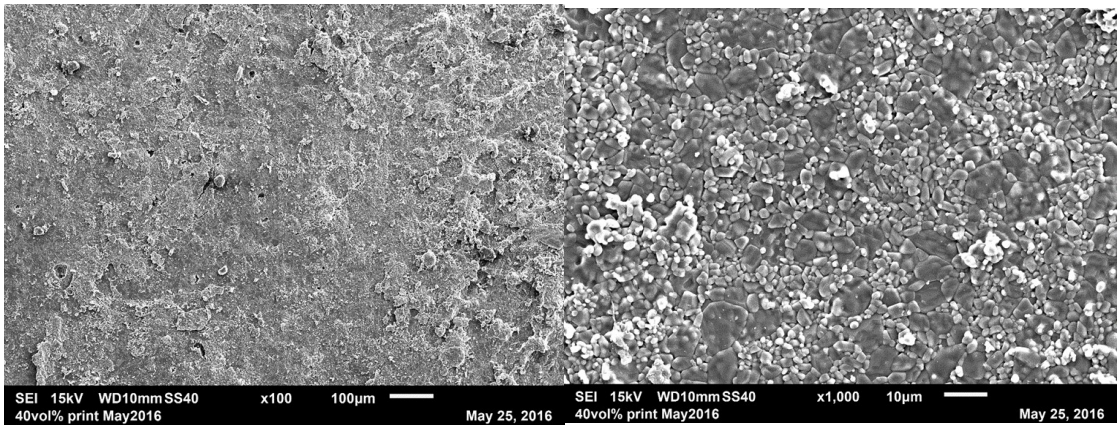

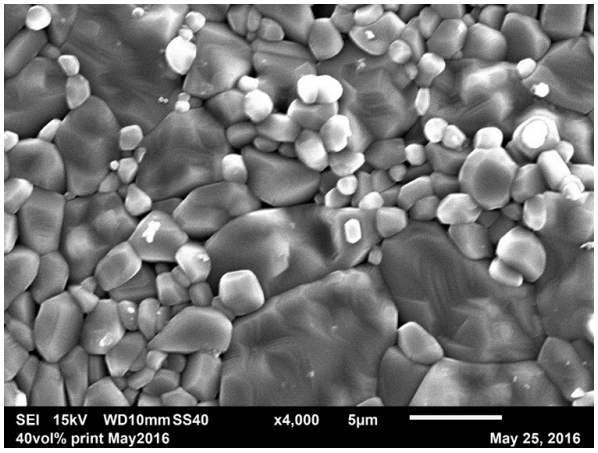

Figure 4.7.7: SEM images of print 4 (94% relative density). Grain range measured 0.58µm to 16µm.

The microstructures and densities have shown that the concept of printing a dense ceramic on an off-the-shelf, relatively inexpensive 3D printer is viable. The solid loading of the resin mixture could be further increased by changing the formulation to increase the amount of dispersant and powder, however the issue still remained of the layers being stuck onto the build area window. Until that issue is resolved, I felt that it was irrelevant to make a mixture of 40 or 50 volume % as the sticking issue would still remain. Further work needed to be done to find the proper settings or window coating to prevent the sticking.

Several of the B9 Creator's settings were adjusted in alleviate the issue of the print sticking to the build area window. There were instances where the layers did adhere to the build table, however they eventually fell off resulting in incomplete prints. The incomplete prints were sintered and relative densities ranging from 77% to 94% were measured.

4.8 Teflon Coating Experiments

The PDMS coating on the build area window does not appear to be working well with the alumina loaded resin mixture due to sticking. The Virginia Tech DREAMS website, short for design, research, and education for additive manufacturing systems, discussed how in their stereolithography applications, they use PTFE Teflon to reduce the adhesion of the cured photopolymer to the glass window [39]. Three Teflon products were ordered: Teflon tape, a silicone based lubricant with Teflon aerosol spray, and a Teflon based lubricant aerosol spray.

Figure 4.8.1: Teflon based products that were used to coat the build area window.

The coatings would be evaluated based on their interactions with the resin mixture on an acrylic glass sheet. Ideally the resin should bead on the coated glass much like water beads on a freshly waxed car and glide on the surface with minimal sticking. As shown in Figure 4.8.2, a sheet of acrylic glass was ordered to simulate the build area window, it was divided into four areas: control, silicone spray with Teflon, Teflon tape, and Teflon lubricant.

Figure 4.8.2: Sheet of acrylic glass divided into 4 areas: lubricant with Teflon, control, Teflon tape, silicon spray with Teflon.

First a mixture of photomer and omnirad was prepared, as this was shown to work well with the printer. A few drops were placed into each of the four areas. The mixture spread thinly on all but the Teflon tape, where it beaded.

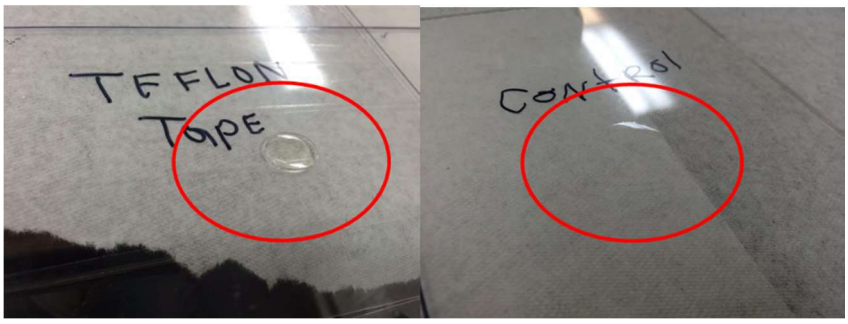

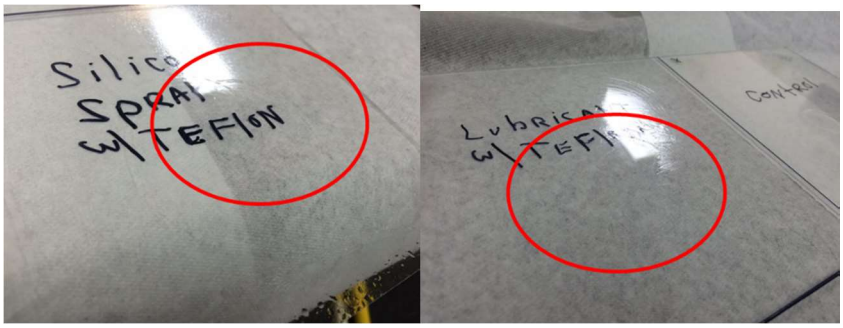

Figure 4.8.3: Photomer + Omnirad mixture placed on the (clockwise from top-left) Teflon tape, control, silicon spray with Teflon, and lubricant with Teflon.

The variquat dispersant was then added to the mixture and the experiment was repeated. Again the mixture spread thinly on all but the Teflon tape. With this information it could be concluded that the dispersant did not affect the interaction between the coating and the resin.

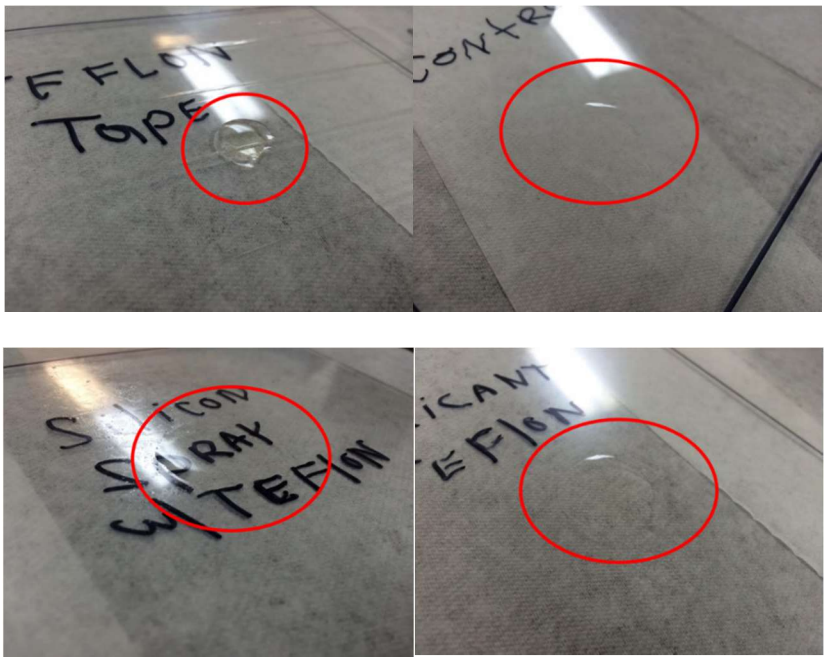

Figure 4.8.4: Photomer + Omirad+ Variquat mixture placed on the (clockwise from top-left) Teflon tape, control, silicon spray with Teflon, and lubricant with Teflon.

Next the alumina powder was added, and the experiment was again repeated. When applied to the four areas, the mixture did not spread out thinly nor did it bead. The glass was tilted to observe how the

mixture flowed. The Teflon tape appeared to allow the mixture to flow more, however there was still a significant amount of sticking that occurred. It became clear that the sticking issue was being caused solely by the addition of the powder.

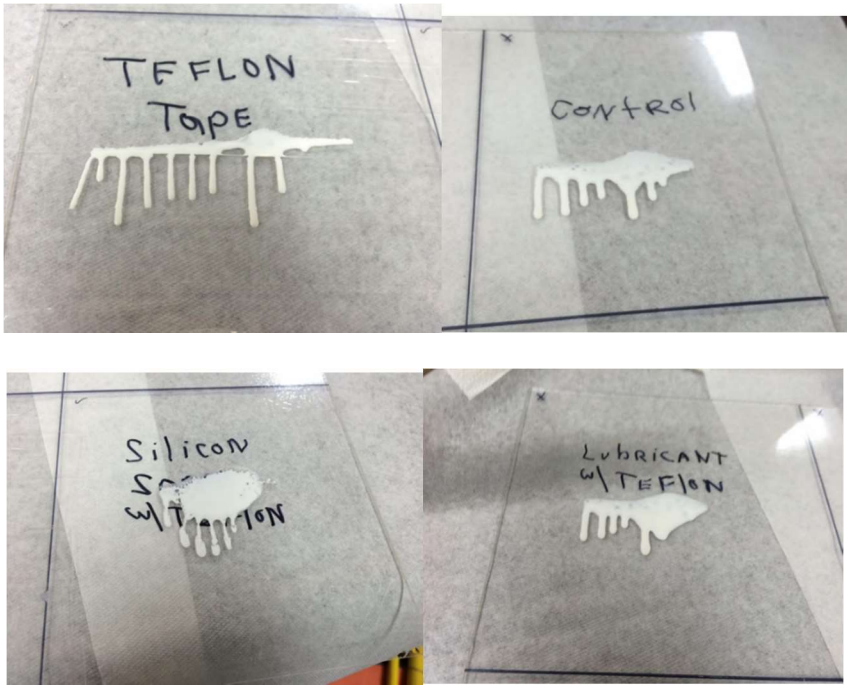

Figure 4.8.5: Photomer + Omnirad + Variquat + Alumina mixture placed on the (clockwise from top-left) Teflon tape, control, silicon spray with Teflon, and lubricant with Teflon.

Several Teflon based products were investigated as a replacement for the PDMS coating on the build area window, with Teflon tape being the most optimistic choice.

4.9 Photoresist Experiments

Another experiment that was performed was using a positive photoresist coating. A photoresist is used in industry to pattern coatings on surface [40]. There are two types of photoresist, a negative photoresist which works by solidifying when exposed to UV light, and a positive photoresist which dissolves when exposed to UV light [40]. The idea, while a long shot, was that the UV light would initiate

the crosslinking in the photopolymer while also dissolving the part of the positive photoresist coating that is also exposed. The dissolved layer would prevent the cured photopolymer layer from sticking to it.

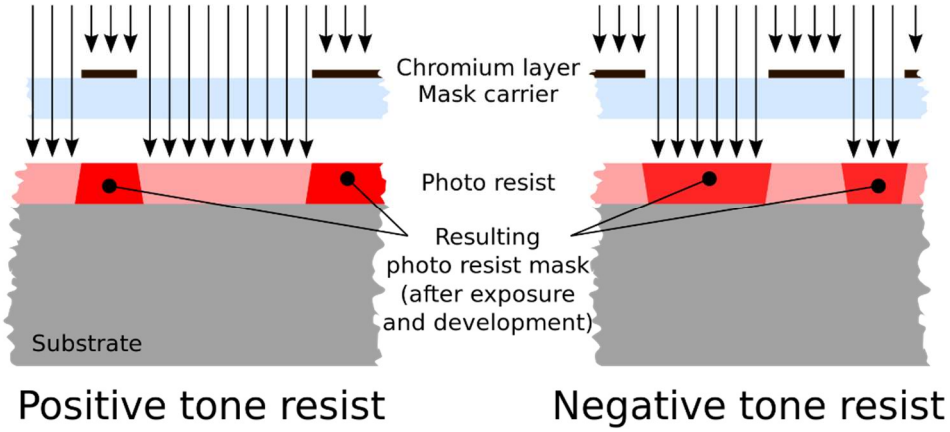

Figure 4.9.1: Image showing the difference between a positive photoresist and a negative photoresist [31].

A positive photoresist was coated onto the build area window using a paintbrush and left to cure overnight at 70 degrees Celsius. The recommended cure time was listed at 90 degrees Celsius, however the vat could not handle that high of a temperature without risk of distorting [26]. The photoresist had a very pungent smell and had to be handled inside of a fume hood. When first applied, the coating had an amber color (Figure 4.9.2), yet after curing the color changed to a dark red-orange (Figure 4.9.3).

Figure 4.9.2: Build area window coated by the positive photoresist.

Figure 4.9.3: Cured positive photoresist coating on build area window.

Drops of the powder loaded mixture were placed on the cured photoresist. Right away it could be seen that the mixture was sticking to the window. The UV light was then applied. The mixture itself began to cure onto the window, and ant attempts to loosen it proved unsuccessful as the photoresist did not show any signs of dissolving.

A positive photoresist was used to coat the build area window as a replacement for the PDMS. The coating proved to be ineffective as powder loaded resin adhered to the coating.

5. Conclusions

The important variables that need to be considered when 3D printing alumina are: viscosity, solid loading, dispersant, photopolymer, and the printer. Without a low enough viscosity the printer would not be able to flow a new layer of photopolymer over the build area window. In order to achieve full densification a high green body density is needed, which is directly related to the solid loading of alumina in the photopolymer. The dispersant coats the powder particles allowing for high solid loadings while maintaining low viscosities. A low viscosity photopolymer is needed that cures at the specific

wavelength of the printer and is miscible with the dispersant. SLA printers use two approaches when building a part, top down in which the build stage builds downwards into the vat, and bottom up where the build stage moves upwards away from the vat. Based on the experiments performed, the best parameters recommended for 3D printing alumina are:

- Viscosity: 281 cP
- Solid loading: 40 volume %
- Dispersant: Quaternary ammonia acetate (Variquat CC-55)
- Photopolymer: Hexanediol diacrylate monomer (Photomer 4017) and photo initiator (Omnirad BL 751)
- Printer: Top-Down

Using the B9 Creator, which was a bottom up printer, a relative density of 94% was achieved from a 40 volume % solid loading of alumina and viscosity of 281 cP. A higher solid loading could be attained by reformulating the concentration of the dispersant in the photopolymer. A top down printer is recommended over the bottom up printer, such as the B9 Creator, because it would eliminate the build area window. Without the window, the sticking issues seen in section 4.7 would be irrelevant. Table 5.1 below shows 7 samples that were sintered. It is important to note that the solid loading of the Dolapix dispersant samples was not correctly measured due to the separation caused between the photopolymer and dispersant, also it did not cure when exposed to UV light. The highest relative density was produced by the Variquat dispersant, however it was inconsistent as the values ranged from 77% to 94%. The grain were also much larger compared to the Silmer dispersant 20 volume % loaded print.

Dispersant	Silmer ACR A0-UP	Dolapix PC 21	Dolapix PC 21 Re-sintered	Variquat CC-55 Print 1	Variquat CC-55 Print 2	Variquat CC-55 Print 3	Variquat CC-55 Print 4
Figure	4.3.10	4.4.3 (left)	4.4.3 (right)	4.7.6	-	-	4.7.7
Resin Volume Solid Loading (%)	20	33*	33*	40	40	40	40
Relative Density (%)	-	88	91	86	77	89	94
Grain Range (μm)	0.17 – 1.60	0.50 – 12	0.5 – 17	0.75 – 20	-	-	0.58 – 16

Table 5.1: Comparison of the 7 sintered samples.

6. Future Work

While a complete, fully dense, printed part was never achieved, we were able to show that an inexpensive plastic printer could be modified to print ceramics, as we were able to partially create some printed parts. The solid loading of the photopolymer could further be increased by adding more powder and more dispersant, followed by high speed mixing. It is not out of the realm to achieve a solid loading of around 60 volume %. The more tricky issues have to do with the printer, the issues that persisted with the B9 printer could potentially be solved by modifying the printer. The printer is very simple with the only moving parts being the build stage and vat. Simple modifications that could be made are to change the sweeper so that the PDMS layer could be exposed to oxygen longer or adding a nozzle that sprays airs onto the PDMS layer to help it oxygenate quicker. The Teflon tape coating showed some promise when placed on the acrylic glass sheet, however we were unable to test it on the actual printer. A challenging modification that could be done would be to invert the printer's projector from the bottom to the top. This would eliminate the need for the glass window since the printer would print directly onto the build stage. Another possible idea would be to determine the charge on the alumina particles through the zeta potential. Once that is known a special vat could be made that would allow for positive or negative charge to be applied to it. By selecting the same charge as the alumina, the particles would

be repelled from the surface of the vat and therefore be less inclined to adhere to it. Finally, the printer could be modified to include ultrasonic agitation so that the powder does not fall out of suspension.

7. References

[1] Schoffer, Filemon. "How Expiring Patents Are Ushering in the Next Generation of 3D Printing." *Tech Crunch*. N.p., 15 May 2016. Web.

[2] Hornick, John, and Dan Roland. "Many 3D Printing Patents Are Expiring Soon: Here's a Round Up and Overview of Them." *3D Printing Industry*. N.p., 29 Dec. 2013. Web.

[3] http://www.aniwaa.com/product/3d-printers/lithoz-cerafab-7500/

[4] De Guire, Eileen. "Ceramics in Electronics." *Ceramics.org*. The American Ceramic Society, 19 May 2014. Web.

[5] AZoM. "Ceramics in Modern Dentistry." *AZoM.com*. AZO Materials, 16 May 2002. Web

[6] Pwray@ceramics.org. "Structure and Properties of Ceramics." *Ceramics.org*. The American Ceramic Society, 21 May 2014. Web.

[7] Yoo, J., M.J Cima, S. Khanuja, and E.M Sachs. *Structural Ceramic Components by 3D Printing*. Tech. Cambridge: Massachusetts Institute of Technology, n.d. Print.

[8] Hagedorn, Yves-Christian. *Additive Manufacturing of High Performance Oxide Ceramics via Selective Laser Melting*. Diss. Aachen U, 2013

[9] C. Sun, X. Zhang, The influences of the material properties on ceramic microstereolithography, Sensors and Actuators A: Physical 101 (2002) 364–370

[10] AZoM. "Cold Isostatic Pressing, Hot Isostatic Pressing and Sinter-HIP'ing." *Azom.com*. Azo Materials, 11 July 2002. Web.

[11] Melcher R, Martins S, Travitzky N, Greil P. Fabrication of Al2O3- based composites by indirect 3D-printing. Mater Lett 2006;60(4):572–5.

[12] S. Maleksaeedi, et al., Property enhancement of 3D-printed alumina ceramics using vacuum infiltration, J. Mater. Process. Technol. 214 (7) (2014) 1301–1306.

[13] Travitzky N, Bonet A, Dermeik B, Fey T, Filbert-Demut I, Schlier L, et al. Additive manufacturing of ceramic-based materials. Adv Eng Mater 2014; 16(6):729–54.

[14] Dolenc, A. "An Overview of Rapid Prototyping Technologies In Manufacturing." Diss. Helsinki U of Technology, 1994. Penn State University. Web. < http://citeseerx.ist.psu.edu/viewdoc/download?doi=10.1.1.106.9496&rep=rep1&type=pdf>.

[15] P. Bertrand, et al., Ceramic components manufacturing by selective laser sintering, Appl. Surf. Sci. (2007), doi:10.1016/j.apsusc.2007.08.085

[16] Klocke, F, and Ader, C., (2003) “Direct Laser Sintering of Ceramics,” Proceedings of Solid Freeform Fabrication Symposium, Austin, Texas, pp. 447-455

[17] Palmero, Elizabeth. "What Is Laminated Object Manufacturing." *LiveScience.com*. Live Science, 9 Oct. 2013. Web.

[18] "The History of Stereolithography (SLA)." *Intechrp.com*. In'Tech Industries, 14 Jan. 2014. Web. <http://www.intechrp.com/the-history-of-stereolithography-sla/>.

[19] Griffith, M.L. and J. W. Halloran, 1994, "Ultraviolet Curing of Highly Loaded Ceramic Suspensions for Stereolithography of Ceramics," Solid Freeform Fabrication Symposium, Austin, TX., pp. 396-403.

[20] Chartier, T., Chaput, C., Doreau, F. and Louseau, M., Stereolithography of structural complex ceramic parts. J. Mater. Sci., 2002(37), 3141–3147.

[21] Goffard, R., Sforza, T., Clarinval, A., Dormal, T., Boilet, L., Hocquet, S., and Cambier, F.: Additive manufacturing of biocom-patible ceramics, Advances in Production Engineering & Management, Vol. 8, no. 2, p.p. 96–106, 2013.

[22] Molitch-Hou, Michael. "First Low Cost SLS 3D Printers Hit the Scene." *3dprintingindustry.com*. 3D Printing Industry, 14 Aug. 2014. Web.

[23] http://www.solidmodelusa.com/collections/solido

[24] http://www.aniwaa.com/product/3d-printers/3dceram-ceramaker/

[25] Krassenstein, Brian. "Judge Rules in Favor of 3D Systems in Resin Based Antitrust Case with DSM Desotech." *3dprint.com*. 3DR Holdings, 21 May 2014. Web.

[26] https://www.b9c.com/

[27] https://www.b9c.com/forum/viewtopic.php?t=301

[28] Blamire, John. "The Giant Molecules of Life: Monomers and Polymers." *Brooklyn.cuny.edu*. The City University of New York, 1997. Web.

[29] https://www.sigmaaldrich.com/content/dam/sigma-aldrich/docs/Aldrich/General_Information/photoinitiators.pdf

[30] G. Allen Brady, John W. Halloran, (1997) "Stereolithography of ceramic suspensions", Rapid Prototyping Journal, Vol. 3 Iss: 2, pp.61 – 65

[31] http://www.engineeringtoolbox.com/absolute-viscosity-liquids-d_1259.html

[32] J. Deckers, J. Vleugels, J.P. Kruthl, Additive manufacturing of ceramics: a review, J. Ceram. Sci. Technol. 5 (2014) 245–260.

[33] Beetsma, Jochum. "The Differences Between Wetting Agents and Dispersants." *Knowledge.ulprospector.com*. Prospector, 10 Apr. 2015. Web.

[34] Cesarano III, J. and Aksay, I. A., Stability of aqueous aalumina suspensions stabilised with polyelectrolytes. J. Am. Ceram. Soc., 1988, 71(12), 1062±1067.

[35] https://americas.sartomer.com/techlitdetail.asp?plid=1&sgid=6&prid=SR415

[36] https://www.ulprospector.com/en/eu/Adhesives/Detail/4958/203149/Irgacure-819-DW

[37]http://www.chemicalland21.com/industrialchem/functional%20Monomer/ETHYLENE%20GLYCOL%20DIMETHACRYLATE.htm

[38] https://www.b9c.com/forum/viewtopic.php?t=2637

[39] "Mask Projection Stereolithography." *Me.vt.edu*. Virginia Tech, n.d. Web. <http://www.me.vt.edu/dreams/constrained-surface-projection-stereolithography/>.

[40] "Lithography Overviews." *Microchem.com*. Micro Chem, n.d. Web. <http://www.microchem.com/Prod-LithographyOverviewPosNeg.htm>.

[41] http://www.lithoz.com/en/

[42] 3D Printing Industry. "The Free Beginner's Guide." *3dprintingindustry.com*. 3D Printing Industry, n.d. Web. <https://3dprintingindustry.com/3d-printing-basics-free-beginners-guide/processes/>.

[43] A. Ambrosi, M. Pumera, 3D-printing technologies for electrochemical applications, Chem. Soc. Rev. (2016)